One-Step Gas–Solid-Phase Diffusion-Induced Elemental Reaction for Bandgap-Tunable $Cu_aAg_{m1}Bi_{m2}I_n$/CuI Thin Film Solar Cells

Erchuang Fan[1, 2], Manying Liu[1, *], Kangni Yang[1], Siyu Jiang[1, 2], Bingxin Li[1], Dandan Zhao[1], Yanru Guo[1], Yange Zhang[1], Peng Zhang[2], Chuantian Zuo[3], Liming Ding[3, *] and Zhi Zheng[1, 2, *]

[1] Key Laboratory of Micro-Nano Materials for Energy Storage and Conversion of Henan Province, Institute of Surface Micro and Nano Materials, College of Chemical and Materials Engineering, Xuchang University, Xuchang 461000, P. R. China

[2] School of Materials Science and Engineering, Zhengzhou University, Zhengzhou 450001, P. R. China

[3] Center for Excellence in Nanoscience (CAS), Key Laboratory of Nanosystem and Hierarchical Fabrication (CAS), National Center for Nanoscience and Technology, Beijing 100190, P. R. China

*Corresponding authors: E-mail: manyingliu988@xcu.edu.cn (M. Y. Liu); ding@nanoctr.cn (L. M. Ding); zzheng@xcu.edu.cn (Z. Zheng)

Supplementary Figures and Tables

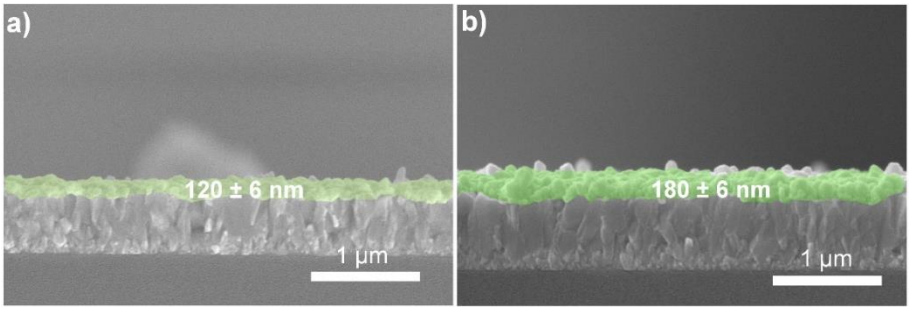

Fig. S1 Cross-sectional SEM of sputtered Bi layers of (a)120 nm and (b) 180 nm

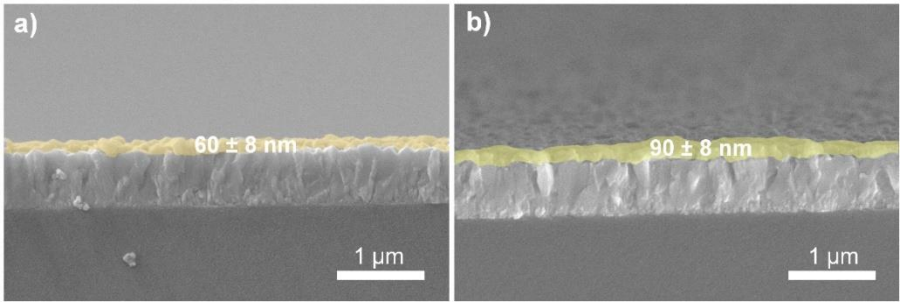

Fig. S2 Cross-sectional SEM of sputtered Cu layers of (a) 60 nm and (b) 90 nm

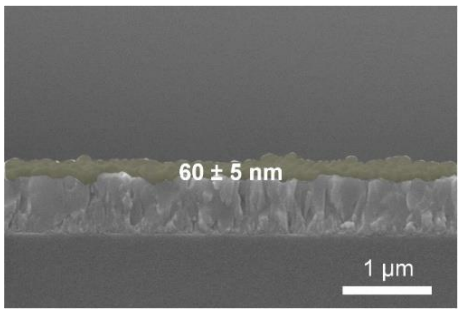

Fig. S3 Cross-sectional SEM of sputtered Ag layers of 60 nm

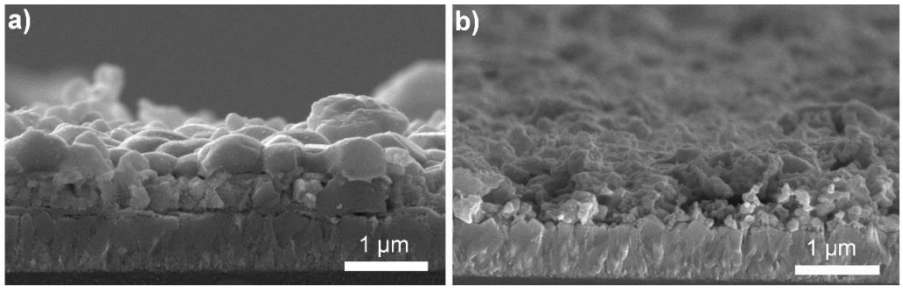

Fig. S4 Cross-sectional SEM images of the $Cu_{0.6}AgBi_2I_{7.6}$ film (a) before and (b) after etching by HNO_3

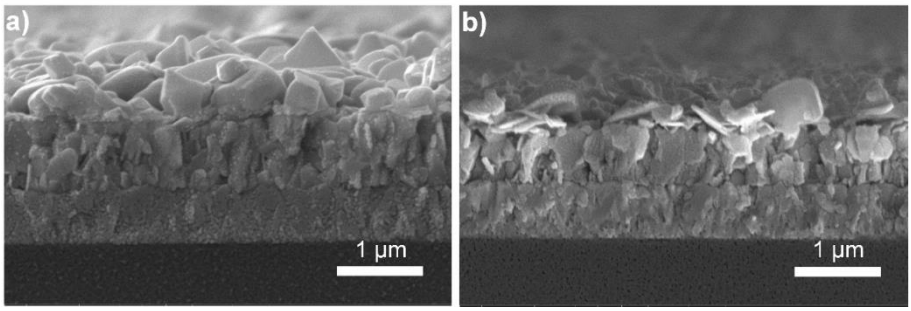

Fig. S5 Cross-sectional SEM images of the $Cu_{0.7}AgBi_2I_{7.7}$ film (a) before and (b) after etching by HNO_3

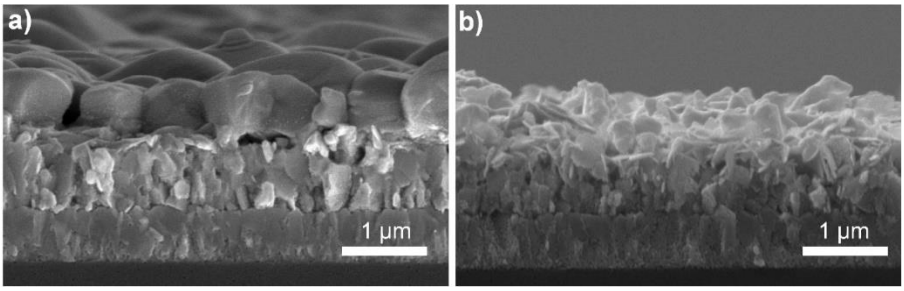

Fig. S6 Cross-sectional SEM images of the $CuAgBi_2I_8$ film (a) before and (b) after etching by HNO_3

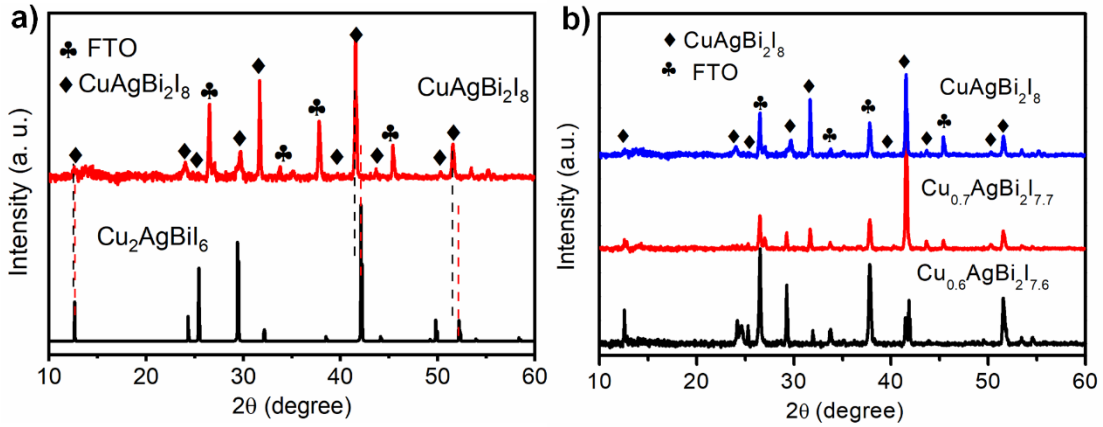

Fig. S7 XRD patterns of (a) $CuAgBi_2I_8$ and Cu_2AgBiI_6, and (b) $Cu_{0.6}AgBi_2I_{7.6}$, $Cu_{0.7}AgBi_2I_{7.7}$, and $CuAgBi_2I_8$ after etching

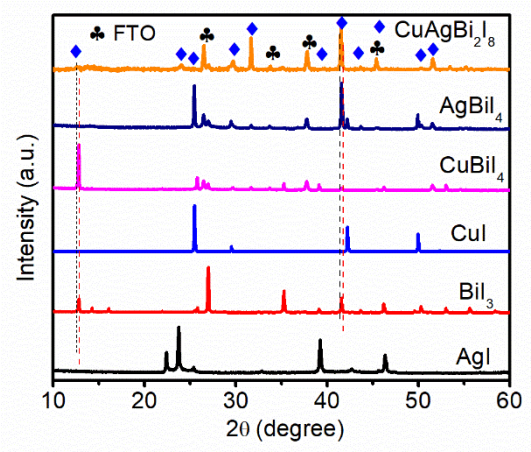

Fig. S8 XRD patterns of $CuAgBi_2I_8$, $AgBiI_4$, $CuBiI_4$, CuI, BiI_3 and AgI

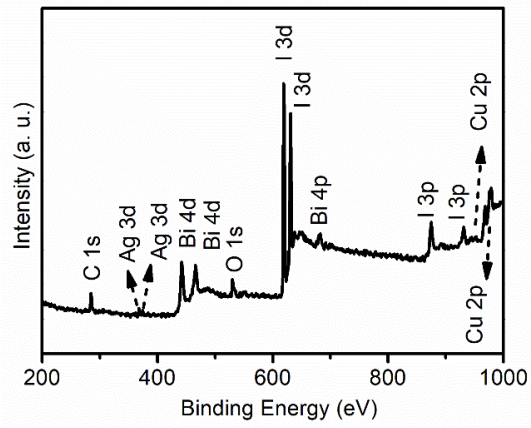

Fig. S9 High resolution XPS spectra of $CuAgBi_2I_8$

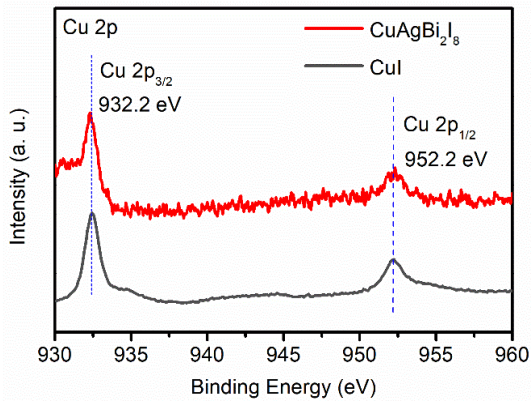

Fig. S10 High resolution XPS spectra of Cu 2p in $CuAgBi_2I_8$ and CuI

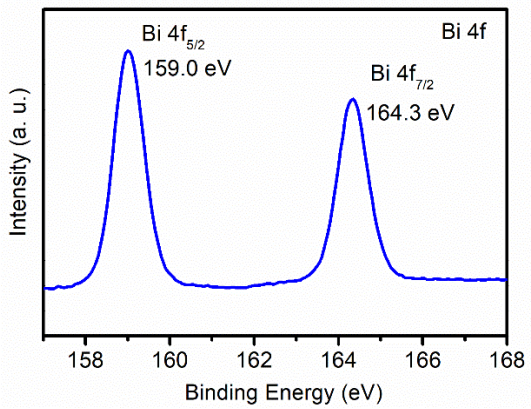

Fig. S11 High resolution XPS spectra of Bi 4f in $CuAgBi_2I_8$

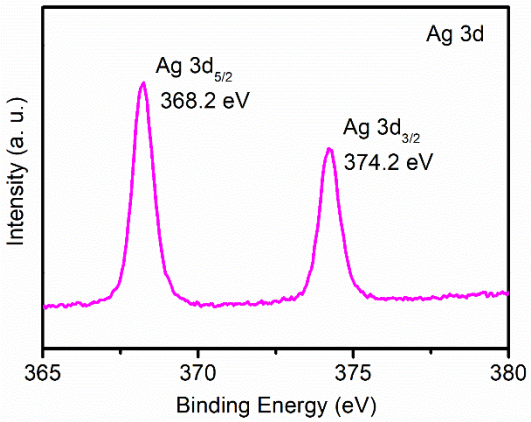

Fig. S12 High resolution XPS spectra of Ag 3d in $CuAgBi_2I_8$

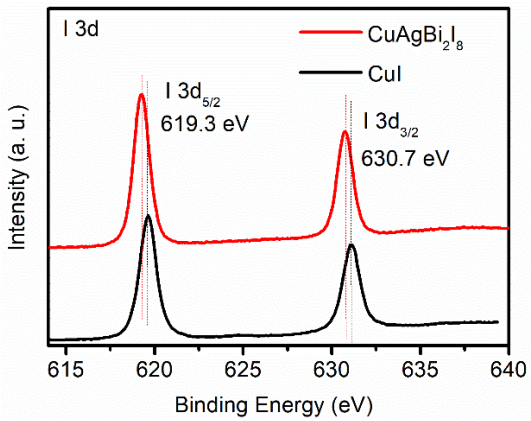

Fig. S13 High resolution XPS spectra of I 3d in $CuAgBi_2I_8$ and CuI

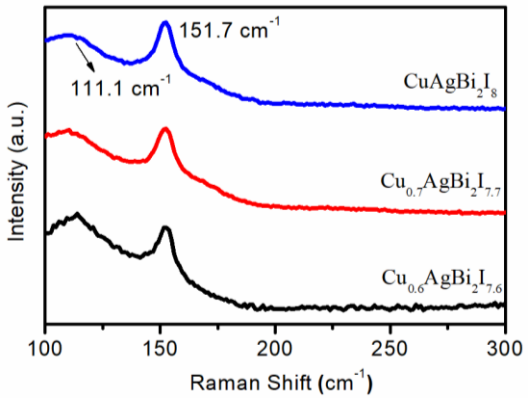

Fig. S14 Raman spectra of $Cu_{0.6}AgBi_2I_{7.6}$, $Cu_{0.7}AgBi_2I_{7.7}$ and $CuAgBi_2I_8$ thin films

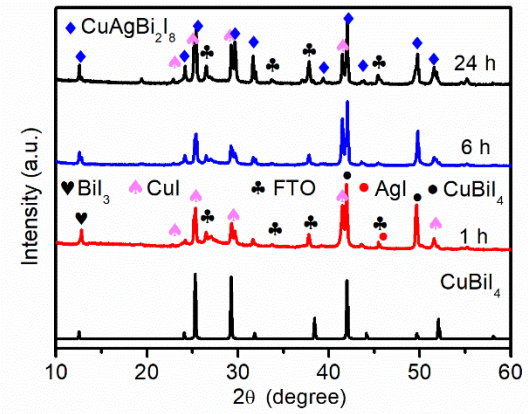

Fig. S15 XRD patterns of $CuAgBi_2I_8$ compounds at different reaction time

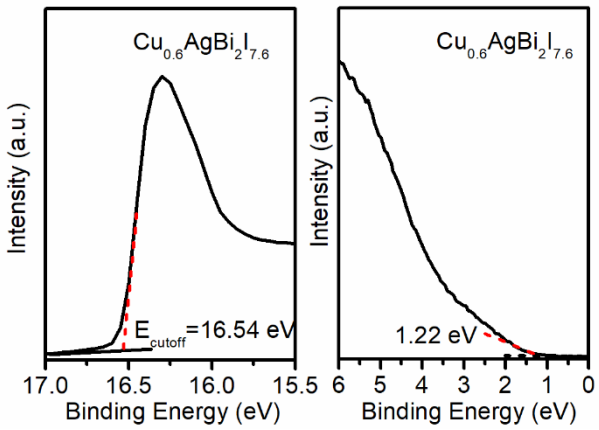

Fig. S16 UPS spectra of $Cu_{0.6}AgBi_2I_{7.6}$

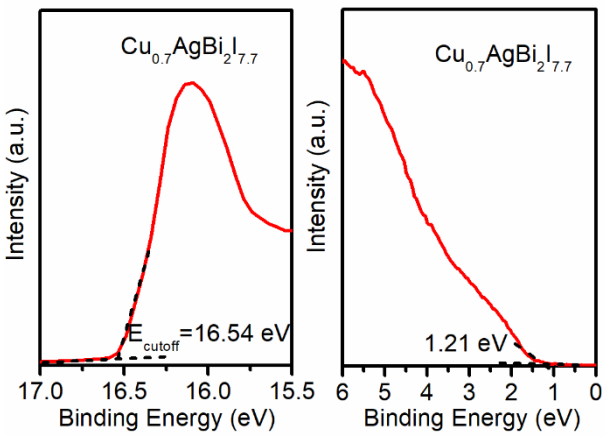

Fig. S17 UPS spectra of $Cu_{0.7}AgBi_2I_{7.7}$

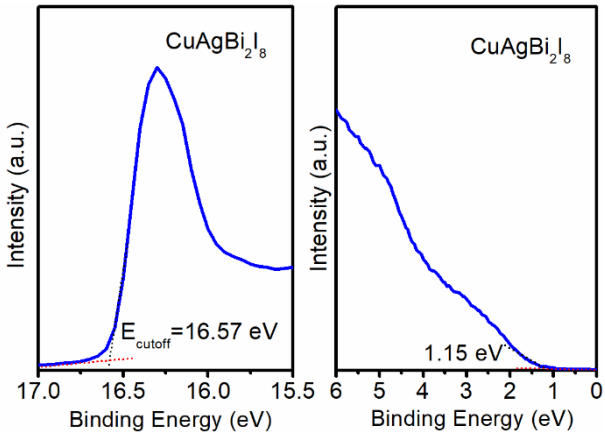

Fig. S18 UPS spectra of $CuAgBi_2I_8$

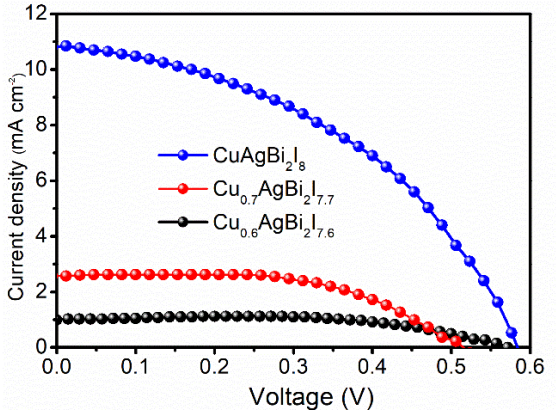

Fig. S19 J-V curve of $Cu_{0.6}AgBi_{2.0}I_{7.6}$, $Cu_{0.7}AgBi_2I_{7.7}$, and $CuAgBi_2I_8$ solar cells

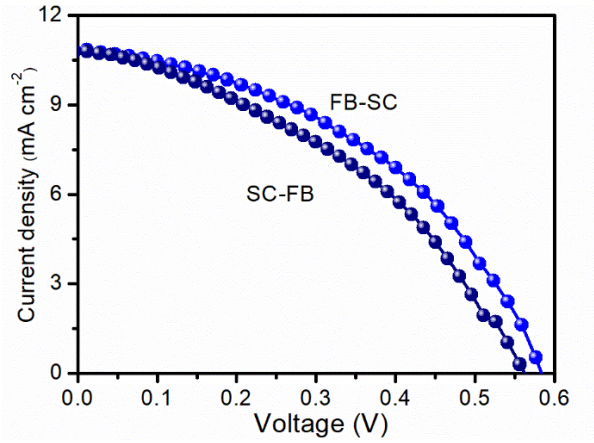

Fig. S20 J–V curves measured using $CuAgBi_2I_8$ devices under reverse and forward voltage scans at AM 1.5G illumination with a scan rate of $1 \cdot V \cdot s^{-1}$

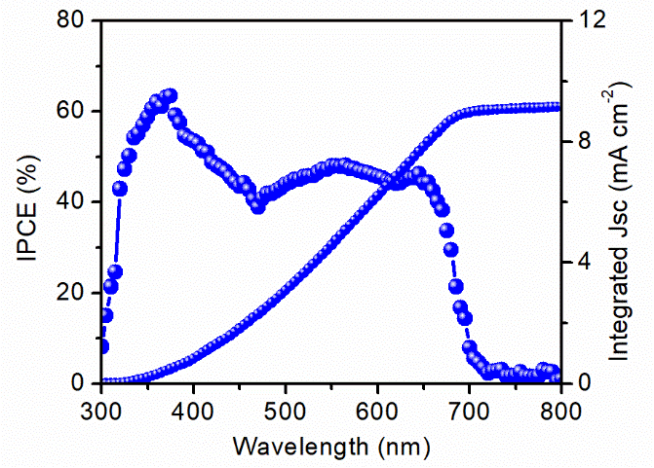

Fig. S21 The IPCE spectra and integrated photocurrent of $CuAgBi_2I_8$ device

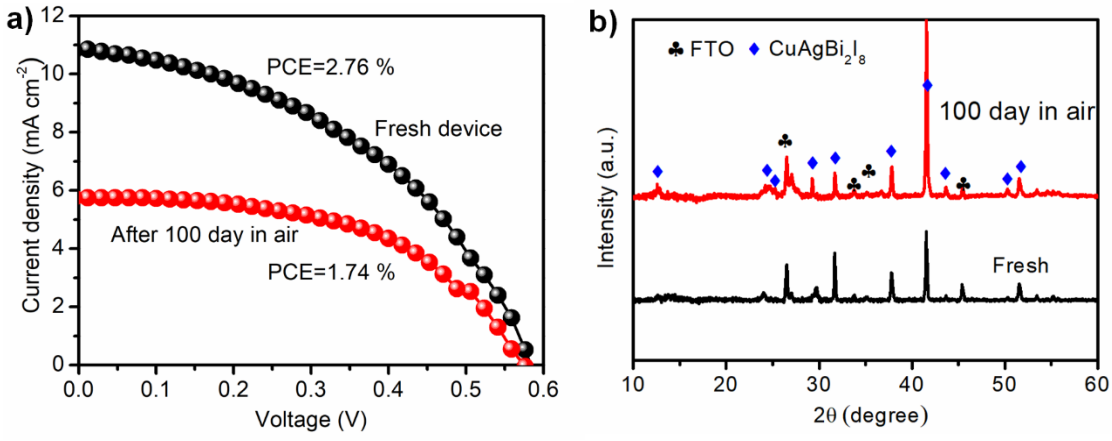

Fig. S22 (a) The J-V curves of fresh $CuAgBi_2I_8$ device and $CuAgBi_2I_8$ devices after 100 days in air. (b) XRD patterns of fresh $CuAgBi_2I_8$ and $CuAgBi_2I_8$ film after 100 days in air

Table S1 The Cross-sectional atomic ratios of $Cu_{0.6}AgBi_2I_{7.6}$/CuI from EDS analysis

	Region	Cu (At%)	Ag (At%)	Bi (At%)	I (At%)
Top layer	1	1.0	0.11	0.00	0.96
	2	1.0	0.17	0.00	1.1
	3	1.0	0.13	0.00	0.94
	Average	1.0	0.14 ± 0.03	0.00	1.0 ± 0.1
Bottom layer	1	0.66	1.0	2.1	6.0
	2	0.52	1.0	2.1	5.4
	3	0.55	1.0	1.9	5.4
	Average	0.60 ± 0.08	1.0	2.0 ± 0.1	5.6 ± 0.4

Table S2 The Cross-sectional atomic ratios of $Cu_{0.7}Ag_{1.00}Bi_{2.00}I_{7.7}$/CuI from EDS analysis

	Region	Cu (At%)	Ag (At%)	Bi (At%)	I (At%)
Top layer	1	1.0	0.07	0.00	1.0
	2	1.0	0.07	0.00	1.0
	3	1.0	0.09	0.00	1.1
	Average	1.0	0.07 ± 0.02	0.00	1.0 ± 0.1
Bottom layer	1	0.75	1.0	1.9	5.9
	2	0.75	1.0	2.0	5.7
	3	0.68	1.0	2.1	6.1
	Average	0.70 ± 0.08	1.0	2.0 ± 0.1	5.9 ± 0.2

Table S3 The cross-sectional atomic ratios of $CuAgBi_2I_8$/CuI from EDS analysis

	Region	Cu (At%)	Ag (At%)	Bi (At%)	I (At%)
Top layer	1	1.0	0.06	0.00	1.1
	2	1.0	0.05	0.00	1.1
	3	1.0	0.04	0.00	0.94
	Average	1.0	0.05 ± 0.01	0.00	1.1 ± 0.1

Bottom layer	1	0.97	1.0	2.2	6.0
	2	0.86	1.0	1.8	5.5
	3	1.1	1.0	2.0	6.2
	Average	1.0 ± 0.1	1.0	2.0 ± 0.2	5.9 ± 0.3

Table S4 ICP analysis of $Cu_aAg_{m1}Bi_{m2}I_n$

$Cu_aAg_{m1}Bi_{m2}I_n$	Cu (mol/L)	Cu (At%)	Ag (mol/L)	Ag (At%)	Bi (mol/L)	Bi (At%)	I (mol/L)	I (At%)
$Cu_{0.6}AgBi_2I_{7.6}$	0.70×10^{-4}	5.00	1.2×10^{-4}	8.57	2.4×10^{-4}	17.1	0.97×10^{-3}	69.4
$Cu_{0.7}AgBi_2I_{7.7}$	1.1×10^{-4}	5.91	1.6×10^{-4}	8.60	2.9×10^{-4}	15.6	1.3×10^{-3}	69.8
$CuAgBi_2I_8$	1.5×10^{-4}	9.70	1.3×10^{-4}	8.41	2.7×10^{-4}	17.4	1.0×10^{-3}	64.5

Table S5 The atomic ratios of $Cu_aAg_{m1}Bi_{m2}I_n$ from XPS analysis

$Cu_aAg_{m1}Bi_{m2}I_n$	Cu (At%)	Ag (At%)	Bi (At%)	I (At%)
$Cu_{0.6}AgBi_2I_{7.6}$	10.52	18.73	34.78	35.98
$Cu_{0.7}AgBi_2I_{7.7}$	8.000	11.83	24.13	56.04
$CuAgBi_2I_8$	10.08	10.52	24.37	55.03

Table S6 Fitting parameters of the TRPL spectra for $Cu_aAg_{m1}Bi_{m2}I_n$ thin film

$Cu_aAg_{m1}Bi_{m2}I_n$	A_1	τ_1 (ns)	A_2	τ_2 (ns)	τ_{ave} (ns)
$Cu_{0.6}AgBi_2I_{7.6}$	0.430	143	0.500	39.6	81.3
$Cu_{0.7}AgBi_2I_{7.7}$	0.550	162	0.420	46.9	109
$CuAgBi_2I_8$	0.580	299	0.370	73.2	201

Table S7 The TSPV parameters of $Cu_aAg_{m1}Bi_{m2}I_n$ thin film

$Cu_aAg_{m1}Bi_{m2}I_n$	V_{max} (V)	T_t (s)	T_r (s)	T_t/T_r
$Cu_{0.6}AgBi_2I_{7.6}$	1.51	5.23×10^{-7}	3.16×10^{-4}	1.66×10^{-3}

$Cu_{0.7}AgBi_2I_{7.7}$	2.31	1.03×10^{-6}	2.91×10^{-3}	3.54×10^{-4}
$CuAgBi_2I_8$	7.57	9.59×10^{-7}	5.48×10^{-3}	1.75×10^{-4}

Table S8 The parameters of $CuAgBi_2I_8$ from Hall effect experiment

Sample	Resistivity (ohm·cm)	Hall coefficient ($cm^3 C^{-1}$)	Carrier concentration (cm^{-3})	Mobility ($cm^2 v^{-1} s^{-1}$))
$CuAgBi_2I_8$	1.58×10^4	4.44×10^4	1.41×10^{14}	2.80

Table S9 Photovoltaic parameters for FTO/c-TiO_2/m-TiO_2/$Cu_aAg_{m1}Bi_{m2}I_n$/CuI/C solar cells under AM 1.5 G irradiation

Sample	V_{oc} (V)	J_{sc} (mA/cm^2)	FF (%)	PCE (%)
$Cu_{0.6}AgBi_2I_{7.6}$	0.571	1.02	63.6	0.371
$Cu_{0.7}AgBi_2I_{7.7}$	0.510	2.62	67.4	0.902
$CuAgBi_2I_8$	0.582	10.8	43.7	2.76